CrossMark

RESEARCH PAPER

Activation of Antigen-Specific CD8$^+$ T Cells by Poly-DL-Lactide/Glycolide (PLGA) Nanoparticle-Primed Gr-1^{high} Cells

Wen-Hui Luo[1] · Ya-Wun Yang[1]

ABSTRACT

Purpose The aim of this study was to investigate the induction of antigen-specific T cell activation and cell cycle modulation by a poly-DL-lactide/glycolide (PLGA) nanoparticle (NP)-primed CD11b$^+$Gr-1^{high} subset isolated from mouse bone marrow.

Methods PLGA NPs containing the ovalbumin (OVA) antigen were prepared using the double emulsion and solvent evaporation method, and protein release rate and cell viability were determined. The Lin2$^-$CD11b$^+$Gr-1^{high}Ly6c^{low} (Gr-1^{high}) subset was sorted from the bone marrow of C57BL/6 J mice by fluorescence-activated cell sorting (FACS) and co-cultured with OT-I CD8$^+$ splenic T cells. Proliferation of OT-I CD8$^+$ T cells was monitored, and cell cycles were determined by 5-bromo-2′-deoxyuridine (BrdU) labeling.

Results Treatment of Gr-1^{high} cells with PLGA/OVA NPs upregulated expression of the SIINFEKL-H2K^b complex in the context of MHC I. Co-cultures of OT-I CD8$^+$ T cells with the PLGA/OVA NP-primed Gr-1^{high} cells induced the proliferation of T cells *in vitro* and modulated cell division and morphology. Treatment of Gr-1^{high} cells with PLGA/OVA NPs also induced cell apoptosis and necrosis.

Conclusion This study demonstrated the function of PLGA/OVA NPs in the activation of OT-I CD8$^+$ T cells and the capability of cross-presentation via the Gr-1^{high} polymorphonuclear subset from mouse bone marrow.

✉ Ya-Wun Yang
  ywyang@ntu.edu.tw

[1] School of Pharmacy, College of Medicine, National Taiwan University, 33 Linsen South Road, Taipei City 10050, Taiwan

ABBREVIATIONS

7-AAD	7-amino-actinomycin D
ACK	ammonium-chloride-potassium
BrdU	bromo-deoxyuridine
CFSE	5-(and-6)-carboxyfluorescein diacetate, succinimidyl ester
CTL	cytotoxic T lymphocyte
MHC	major histocompatibility complex
NPs	nanoparticles
OVA	ovalbumin
PLGA	poly(lactide-co-glycolide)
PMN	polymorphonuclear neutrophils

INTRODUCTION

The development of effective cancer vaccines for the generation of cellular immunity is important for protecting the host against cancers. Dendritic cells are considered the most powerful antigen presenting cells (APCs) in anti-tumor immune responses by presenting the tumor antigens to the CD8$^+$ T cells in cancer immunotherapy. Previous studies have shown that stimulation of T cell receptor (TCR) by antigen presenting cells expressing the cognate antigen in the context of MHC I is able to activate antigen-specific effector CD8$^+$ T cells and induce cellular division and expansion (1). Therefore, these processes have been targeted by several groups in vaccine-based cancer therapy to boost the anti-tumor response by activation of antigen-specific cytotoxic T cells, which are critical for the generation of antitumor immune responses and the development of effective cancer vaccines (2, 3).

Nanoparticles (NPs) made from biodegradable polymers, such as poly-DL-lactide/glycolide (PLGA), emerged as an interesting drug delivery system not only in the field of pharmaceutical sciences but also in vaccine development for the

enhancement of adaptive immunity (4, 5). In an attempt to modulate the adaptive immune system, strategies in vaccine research have been developed by engineering the biomaterials such that antigens can be delivered through specific cellular pathways (6). In nanoparticle-based vaccine delivery, the particles were utilized as carriers to deliver antigens to the antigen presenting cells (APCs) to trigger the antigen-specific T cell response (7–10). Major scientific efforts on antigen delivery and presentation in the past few years have been made by targeting dendritic cells, B cells, and macrophages or the myeloid subsets employing polymeric nanoparticles for cancer immunotherapy (7, 11, 12). Dendritic cells (DCs), the specialized antigen presenting cells that play pivotal roles in the initiation and modulation of antigen-specific immune responses, have received the most attention as the major target cells for antigen delivery, processing, and presentation to induce protective immunity through the MHC class I or class II pathways (13, 14).

Polymorphonuclear neutrophils (PMN) are the first-line of defense against infective agents. Gr-1 is a granulocyte differentiation antigen expressed in the myeloid linage, including granulocytes (15). The Gr-1^{high} subset of PMNs can migrate from peripheral tissues to the inflammatory sites, phagocytose and clear infective pathogens. Despite their relatively high phagocytic capability, these cells have been largely ignored in regard to their roles in antigen presentation due to the lack of expression of major histocompatibility complex (MHC) class II antigens and costimulatory molecules such as CD80 or CD86. Although dendritic cells are recognized as the most effective antigen presenting cells for cross presentation (16–18), recent studies have demonstrated the capability of granulocytic neutrophils to cross-prime T cells *in vivo* (19). In our previous studies, we have also demonstrated the infiltration of leukocytes to the vaccine adjuvant-injection sites to uptake antigens (20). These data raised the potential target of bone marrow granulocytes in nanoparticle-based vaccine delivery for the induction of antigen-specific activation of CD8$^+$ T cells. In this study, we evaluated the interactions of polymeric nanoparticles and granulocytes, particularly the CD11b$^+$Gr-1^{high} myeloid subset in mouse bone marrow, to potentially activate antigen-specific CD8$^+$ T cells.

Following antigen activation, T cells undergoing cell division can be analyzed by dilution of carboxyfluorescein diacetate succinimidyl ester (CFSE), a commonly used immunological method to determine cell proliferation both *in vitro* and *in vivo* (21, 22). DNA synthesis in the proliferating cells can also be detected by the use of bromo-deoxyuridine (BrdU) (23, 24). a thymidine analog that can be incorporated into DNA of the cells undergoing S (DNA synthesis) phase to replace thymidine. Cells incorporating BrdU can then be detected with anti-BrdU fluorescent antibodies and analyzed by flow cytometry. The combination of BrdU with 7-amino-actinomycin D (7-AAD) staining allows for determination of cell cycle kinetics

and analysis of cells that are actively synthesizing DNA in their cell cycle position, such as G0/1, S, or G2/M phases (25).

In this study, we aimed to explore whether CD11b$^+$Gr-1^{high} cells are able to acquire soluble antigens from biodegradable PLGA/OVA NPs to activate an antigen-specific CD8$^+$ T cell response and potentially upregulate OVA peptide (257–264) SIINFEKL-MHC I-H2K^b complexes. The results obtained in this study demonstrated that the PLGA/OVA NP-primed CD11b$^+$Gr-1^{high} subset from mouse bone marrow was capable of activating and inducing proliferation of OT-I CD8$^+$ T cells. These data demonstrated explicitly the roles of polymeric nanoparticles containing soluble antigens in triggering the innate immune system and inducing adaptive immunity in the context of MHC class I via the CD11b$^+$Gr-1^{high} subset from the bone marrow.

MATERIALS AND METHODS

Materials

Copolymers of DL-lactide and glycolide (PDLG 5004A; PLGA) (50:50) with MWs of 44,000 kg/mol were kindly provided by Purac (Gorinchem, The Netherlands). The BrdU staining buffer set and 7-AAD viability staining solution were purchased from eBioscience (San Diego, CA). DNase (grade II, bovine pancreatic DNase I) was obtained from Roche Molecular Systems Inc. (Branchburg, NJ). The culture medium was obtained from Hyclone (Logan, Utah). Granulocyte-macrophage colony-stimulating factor (GM-CSF) was purchased from Peprotech (Rocky Hill, NJ). Most fluorochrome-conjugated monoclonal antibodies and their matched isotype controls were purchased from eBioscience (San Diego, CA) or Biolegend (San Diego, CA).

Preparation and Characterization of PLGA/OVA Nanoparticles (NPs)

Preparation of the poly(lactic-co-glycolic acid) (PLGA) nanoparticles (NPs) employing the w/o/w double emulsion and solvent evaporation method was performed similarly to the previously described method (26). Briefly, 20 mg ovalbumin (OVA) was dissolved in 500 μl 2% polyvinyl alcohol (PVA) and mixed with 4.5 ml methylene chloride containing 180 mg of PLDG 5004A (Purasorb). The dispersion was ultrasonicated for 60 s with a Branson Sonifier 450 (Danbury, CT), and 2.5 ml of this dispersion was added to 12.5 ml 2% PVA aqueous solution and homogenized by ultrasonication again for 120 s. The emulsion was then mechanically stirred for 16 h to evaporate off the organic solvent, followed by centrifugation at 12,000 rpm for 10 min with a Beckman J2-21 centrifuge and lyophilized. Samples were kept at −20°C before use. The PLGA/OVA NPs were examined with a

Hitachi S-4800 scanning electron microscope operated at 15 kV.

The mean particle size, the polydispersity index (PDI), and the zeta potential of the PLGA NPs were determined by the quasi-elastic light scattering technique using a Zetasizer Nano ZS (Malvern Instruments Ltd., UK). All data reported are the means of at least three determinations of each preparation.

Animals

C57BL/6 J mice and transgenic OT-I mice, aged 6 to 10 weeks, were used in this study. The OT-I CD8$^+$ T cells recognize the OVA peptide presented by MHC class-I molecules. All animal experiments were performed in accordance with the guidelines of and approved by the Animal Care and Use Committee of our university.

Protein Content in PLGA/OVA NPs and *In Vitro* Release of Ovalbumin

The content of ovalbumin (OVA) in PLGA/OVA NPs was analyzed by placing 10 mg PLGA/OVA NPs in 1 ml 5% sodium dodecyl sulfate (SDS) in 0.1 N NaOH, according to the established method (27, 28). The protein amount in the supernatant was determined 16 h later by spectrophotometry at 562 nm using the bicinchoninic acid (BCA) protein assay kit (Pierce). The encapsulation efficiency and loading percentage were determined based on the following equations (29):

$$\text{Encapsulation efficiency} = (\text{amount of OVA in NPs/initial amount of OVA added}) \times 100\%$$
$$\text{Loading }\% = (\text{amount of OVA entrapped in NPs/total amount of NPs}) \times 100\%$$

The *in vitro* accumulative release of ovalbumin (OVA) from PLGA/OVA NPs was determined by placing 10 mg PLGA/OVA NPs in 0.5 ml PBS in a 37°C shaking water bath. At pre-determined time intervals, the tubes were centrifuged for 10 min at 10,000 rpm, and the supernatant was collected for a protein assay, followed by replacement with fresh buffer of the same volume into the sample tubes.

Viability Assay with 3-(4,5-dimethylthiazol-2-yl)-2,5-diphenyltetrazolium Bromide (MTT)

To determine the dose of PLGA NPs, with or without OVA, for the *in vitro* studies, the viability of primary cells after treatment with PLGA NPs was assessed using the 3-(4,5-dimethylthiazol-2-yl)-2,5-diphenyltetrazolium bromide (MTT) assay as previously described (30, 31). Briefly, bone marrow cells freshly isolated from the femurs and tibiae of C57BL/6 J mice were suspended at 1×10^6/ml in complete RPMI medium, and 100 µl cells were plated in U-bottomed 96-well plates, followed by treatment with various amounts of PLGA NPs for 24 h. Cells were centrifuged and reacted with 20 µl MTT (5 mg/ml) for 2 h, followed by addition of 150 µl dimethyl sulfoxide (DMSO) and incubation for 5 min to dissolve the formazan product. The plates were read at 570 nm with a BioTek Powere Wave XS microplate spectrophotometer (Winooski, VT 05404). Cells treated with PBS served as the 100% viable control. The experiments were performed in triplicate.

Isolation of Lin2⁻CD11b⁺Gr-1^{high} Cells from Bone Marrow and Wright-Giemsa Staining

C57BL/6 J mice were sacrificed after anesthetization with isoflurane. Single cell suspensions from bone marrow were prepared by flushing cells out of the femurs and tibiae of 6- to 10-week old C57BL/6 J mice. Red blood cells were lysed with ammonium chloride–potassium ACK lysing buffer (32). Myeloid CD11b⁺Gr-1⁺ cells were enriched by negative selection with BioMag® goat anti-rat IgG (Qiagen) and anti-mouse Lineage 2 antibody cocktail (CD3/CD19/B220/Ter119/NK1.1) (33) and stained with fluorochrome-conjugated rat anti-mouse antibodies, including Lineage 2 (CD3/CD19/B220/Ter119/NK1.1)-PE, CD11b-PerCP-Cy5.5, Gr-1-FITC, and Ly6C-efluo450, then washed with PBS. The Lin2⁻CD11b⁺Gr-1^{high}Ly6c^{low} (Gr-1^{high}) cells were sorted with a FACSAriaIII cell sorter (BD Biosciences) and cultured in complete RPMI 1640 medium containing 10% fetal bovine serum (FBS), 50 µM 2-mercaptoethanol, 25 mM HEPES, penicillin G (100 U/mL)/streptomycin 100 µg/mL, and 5 ng/ml GM-CSF.

To examine the morphology of the sorted cells, the Lin2⁻CD11b⁺Gr-1^{high}Ly6c^{low} (Gr-1^{high}) cells were centrifuged with a Cytopsin4 (Thermo Scientific) at 1000 rpm for 3 min and collected with silane-coated glass microslides, followed by Wright-Giemsa staining (WG-16, Sigma-Aldrich) and examination with a Zeiss Axio Imager A1 microscope.

Examination of the Uptake of PLGA NPs by the Gr-1^{high} Cells by Microscopy

The sorted Gr-1^{high} cells were treated with PBS or 100 µg/ml PLGA-OVA NPs/PBS and incubated in complete RPMI medium containing 5 ng/ml GM-CSF at 37°C. Cells were harvested 24 h later, re-suspended at 5×10^5 cells/ml in PBS, and cytospun at 1000 rpm for 3 min with a Cytospin4 (Thermo Scientific). Cells were then fixed with methanol and stained with Wright-Giemsa stain, followed by washes with water.

The slides were dried and mounted with DPX mounting medium and examined with a Zeiss Axio Imager A1 microscope.

Generation of Bone Marrow-Derived Dendritic Cells

Bone marrow derived dendritic cells (BMDCs) were prepared as previously described (20, 34, 35). Briefly, bone marrow cells were collected by flushing cells from femurs and tibias of C57BL/6 mice. Red blood cells were depleted with ACK lysis buffer (0.15 M NH$_4$Cl, 1.0 mM KHCO$_3$, 0.1 mM Na$_2$EDTA) (36). Cells were cultured in the multi-well plates in the complete RPMI 1640 medium, supplemented with recombinant mGM-CSF and mIL-4, and the medium was replaced every 2 days. The non-adherent cells were collected on day 6 and were used in subsequent experiments.

Preparation of CD8$^+$ T Cells from the Spleen of OT-I Mice

Murine splenocytes were freshly isolated from transgenic MHC class I-restricted TCR (OT-I) mice, and single cell suspensions were prepared. Red blood cells were removed by the ACK (ammonium-chloride-potassium) lysing buffer, washed with PBS, and enriched by incubation at 4°C for 30 min with antibody cocktails containing I-A/I-E (M5/114.15.2), Ter-119, B220 (RA3-6B2), CD11b (M1/70), Gr-1 (RB6-8C5), CD44 (IM7.81), CD4 (GK1.5), and CD19 (1D3). Cells were washed again with PBS/1% fetal bovine serum (FBS) and incubated with BioMag® goat anti-rat IgG (Qiagen) microbeads at 4°C for 20 min according to the manufacturer's instructions, followed by magnetic separation with a Miltenyi magnetic separation stand. The unadsorbed cells were collected. The purity of the enriched CD8$^+$ T cells was 81.8%, as assessed by flow cytometric analysis.

Labeling of TCRV$_\beta$5$^+$CD8$^+$ T Cells with 5-(and-6)-carboxyfluorescein Diacetate (CFSE) and Proliferation *In Vitro*

The Lin2$^-$CD11b$^+$Gr-1^{high}Ly-6C^{low} (Gr-1^{high}) cells were treated with PBS, 10 µg/ml OVA, PLGA NPs (100 µg/ml), or PLGA/OVA NPs (100 µg/ml) and incubated at 37°C for 16 h. The CD8$^+$ cells that were enriched by depletion of unwanted cells, on the other hand, were labeled with 5 µM 5-(and-6)-carboxyfluorescein diacetate, succinimidyl ester (CFSE) for 10 min according to the established protocol (37) and washed with PBS/1% FBS. Activation of antigen-specific T cells was tracked *in vitro* by co-culturing NP-primed Gr-1^{high} cells with CFSE-labeled CD8$^+$ T cells for 72 h, followed by cytometric analysis of proliferation and expression of CD25 and CD69 in TCRV$_\beta$5$^+$CD8$^+$ T cells using a FACSVerse flow cytometer (BD Biosciences).

Examination of the Morphology of Activated T Cells

To examine the effect of NP treatment on the morphology of TCRVα2$^+$CD8$^+$ cells, cells were harvested at the end of co-culture at 72 h and sorted with a BD FACSAriaIII sorter, cytospun onto glass slides, stained with Wright-Giemsa stain, and examined with a Zeiss Axio Imager A1 microscope.

Comparison of the Effect of APCs on the Proliferation of OT-I CD8+ T Cells *In Vitro*

To compare the *in vitro* proliferation of OT-I CD8$^+$ T cells induced by the antigen presenting cells, either day 6 BMDCs or freshly sorted Gr-1^{high} cells (1×10^5/well) were co-cultured at 1:1 in the 96-well plates with CFSE-labeled CD8$^+$ T cells, negatively selected from spleen of the OT-I mouse, followed by treatment with PBS, OVA (10 µg/ml OVA), PLGA NPs (100 µg/ml), or PLGA/OVA NPs (100 ug/ml PLGA/OVA, containing 10 µg/ml OVA). Cells were harvested 72 h later and the division of TCRVβ5$^+$CD8$^+$ T cells were analyzed by flow cytometry.

BrdU Labeling and 7-Amino-Actinomycin D (7-AAD) Staining

To monitor the activation effect of PLGA/OVA NPs on the expansion of antigen-specific T cells via Gr-1^{high} cells, the co-cultured cells were labeled with bromodeoxyuridine (BrdU), followed by staining the cellular DNA with 7-amino-actinomycin D (7AAD). Proliferating T cells were then analyzed with a BD FACSVerse flow cytometer and separated into G1, S, and G2/M subpopulations. To examine the effect of PLGA/OVA NP-primed antigen presenting cells (APCs) on proliferating OT-I CD8$^+$ T cells, the Gr-1^{high} cells were isolated and treated for 16 h with PBS, 10 µg/ml OVA, 100 µg/PLGA NPs, or 100 µg/ml PLGA/OVA NPs and co-cultured for 48 h with CD8$^+$ T cells enriched from the spleen of naive OT-I mice by negative selection, followed by addition of 10 µM BrdU in the culture medium. Cells were further cultured for 24 h at 37°C, harvested, and stained with fluorochrome-conjugated antibodies, including FITC-anti-mouse TCRVα2 (B20.1), APC-Cy7-anti-mouse CD8α (53-6.7), and PE-Cy7-anti-mouse CD3ε (17A2). After staining for 20 min at 4°C, cells were fixed for 20 min with 2% para-formaldehyde/PBS, washed with 1% FBS/PBS, and permeabilized for 15 min with 200 µl 0.1% Triton X-100 (Sigma). Cells were then treated with DNase I (300 µg/ml), incubated at 37°C for 1 h, and stained with APC-conjugated anti-BrdU (BU20A). Next, the addition of 200 µl 0.1% Triton X-100 containing 100 µg/ml RNase A and 5 µg/ml 7-AAD occurred, followed by analysis with a BD FACSVerse cytometer.

Analysis of Apoptosis and Necrosis After Treatment with the PLGA NPs

The Lin2$^-$CD11b$^+$Gr-1^{high}Ly-6C^{low} (Gr-1^{high}) subpopulation was sorted from the bone marrow of C57BL/6 J mice with a BD FACSAriaIII sorter. Cells were plated in 96-well round-bottom microplates at 1×10^5/well and incubated overnight in complete RPMI 1640 medium containing 5 ng/ml GM-CSF and co-cultured with OT-I CD8$^+$ T cells (1×10^5/well), followed by treatment with PBS, 10 μg/ml OVA, 100 μg/ml PLGA NPs, or 100 μg/ml PLGA/OVA NPs (containing 5 μg/ml OVA) at 37°C. Cells were harvested at 24, 36, 48, 60, and 72 h, washed with PBS, and stained with FITC-conjugated anti-Gr-1 mAb. After a 20 min incubation at room temperature, cells were resuspended in 1× Annexin V binding buffer containing Annexin V-PE and incubated for 20 min. Cells were then washed with 1× Annexin V binding buffer, centrifuged, and stained with 7-Aminoactinomycin D (7-AAD) for 5 min, then analyzed with a FACSVerse cytometer (BD Biosciences).

RESULTS

### Scanning Electron Microscopy (SEM) Images of PLGA Nanoparticles

PLGA NPs containing the ovalbumin (OVA) antigen were prepared by the double emulsion-solvent evaporation method as previously described (26). and their morphology is shown in Fig. 1, illustrating that most polymeric nanoparticles are spherical in shape with a diameter of less than one μm (Fig. 1).

Characterization of PLGA Nanoparticles

The mean particle size of PLGA NPs and PLGA/OVA NPs, as determined by dynamic light scattering, are 610.5 ± 11.7 nm and 690 ± 7.1 nm, respectively, and the polydispersity indices (PDI) are 0.21 ± 0.04 and 0.17 ± 0.02, respectively. Zeta potentials of PLGA NPs and PLGA/OVA NPs, on the other hand, were determined to be -26.1 ± 1.2 nm and -30.5 ± 0.5 mV, respectively. The encapsulation and loading percentage (the weight percentage of OVA) in the PLGA/OVA NPs, on the other hand, were determined to be 52.7 ± 1.6 and $5.28 \pm 0.1\%$, respectively.

Cumulative Release of OVA from PLGA/OVA NPs

The *in vitro* release of protein from the OVA-loaded PLGA NPs was performed at 37°C in PBS using the Pierce BCA protein assay kit (Thermo Scientific). The cumulative release curve illustrated a typical sustained
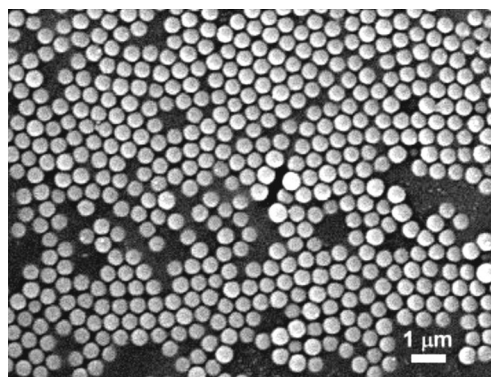

Fig. 1 Scanning electron micrograph of PLGA/OVA NPs, exhibiting the spherical shape and a mean diameter of approximately 690 nm. Scale bar = 1 μm.

release profile of the protein from the polymeric matrix. The initial burst release of proteins occurred within the first 12 h and then leveled off after 120 h, with a maximum release of approximately 60% (Fig. 2).

Determination of the Optimal Dose of Polymeric NPs for the *In Vitro* Experiment Using the MTT Assay

The potential cytotoxic effect of PLGA NPs was evaluated in mouse bone marrow cells using the 3-(4,5-dimethylthiazol-2-yl)-2,5-diphenyltetrazolium bromide (MTT) assay. Figure 3 shows the concentration-dependent cell viability after treatment with the PLGA and PLGA/OVA NPs. Both PLGA and PLGA/OVA NPs elicit insignificant cytotoxic effects below 100 μg/ml, this dose was therefore used in the following *in vitro* experiments. Treatment of cells with PLGA NPs above 300 μg/ml significantly reduced the survival rate.
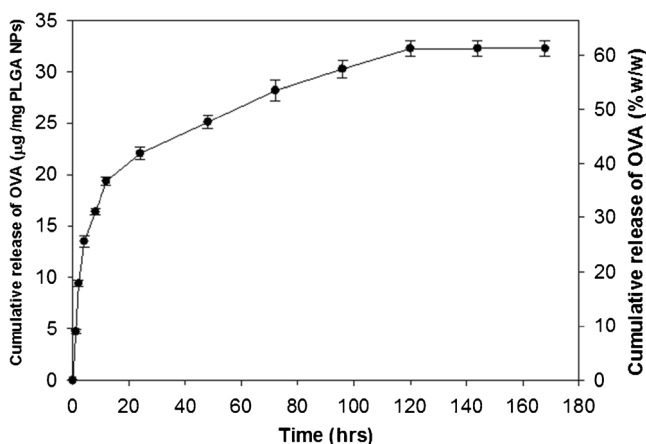

Fig. 2 The cumulative release profile of ovalbumin (OVA) from PLGA/OVA nanoparticles at 37°C. The data are presented as means ± standard error mean (SEM) of three experiments with triplicate samples.
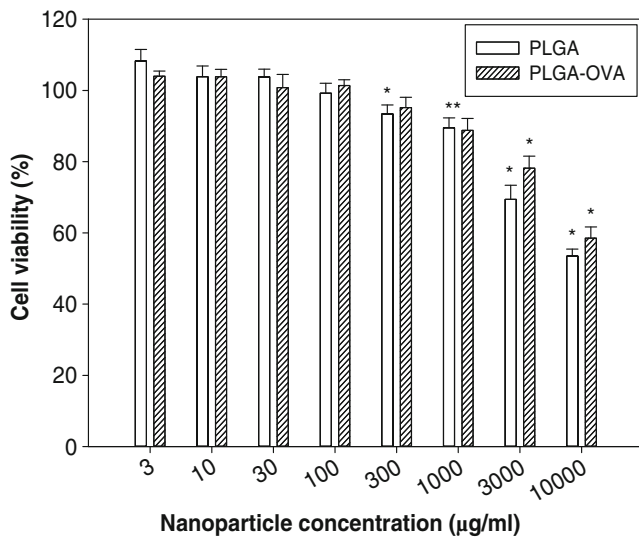
Fig. 3 The MTT viability assay. The percentages of viable cells after treatment with PLGA or PLGA/OVA NPs for 24 h. Freshly isolated bone marrow cells were treated in 96-well microplates with various doses of PLGA or PLGA/OVA NPs for 24 h, followed by reaction with 20 μl of MTT solution (5 mg/ml) for 2 h. The formazan product was dissolved with dimethyl sulfoxide (DMSO), and the absorbance was read at 570 nm. Data are presented as means ± standard error mean (SEM) of three experiments with triplicate wells. *Indicates a statistically significant difference from the PBS-treated control group (*, $P < 0.05$, one-way ANOVA).

Cytometric Analysis of Surface Phenotypes and Microscopic Examination of Morphology of Gr-1^{high} Cells After Sorting by FACS

The Lin2^{−}CD11b^{+}Gr-1^{high}Ly-6C^{low} (Gr-1^{high}) granulocytes (Fig. 4) were sorted from mouse bone marrow and placed at a density of 10^6/ml in complete RPMI-1640 medium supplemented with 5 ng/ml GM-CSF and were treated with or without PLGA/OVA NPs (100 μg/ml) followed by incubation at 37°C for 24 h and photography under the microscope with a Canon EOS 600D camera.
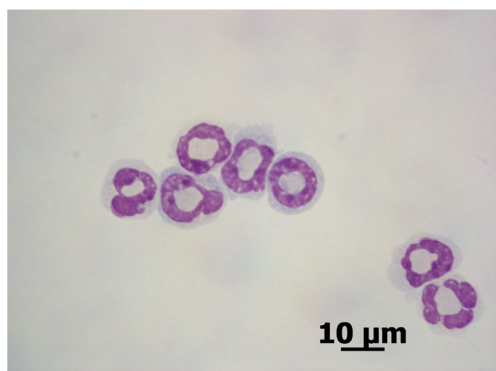

Fig. 4 The Gr-1^{high} (Lin2^{−}CD11b^{+}Gr-1^{high}Ly-6C^{lo}) cells were isolated from bone marrow of tibiae and femurs of mice, stained with fluorochrome-conjugated antibodies against Lin2 (CD3/CD19/NK1.1/B220/Ter119), CD11b, Ly-6C, and Gr-1, and sorted with a BD FACS Aria III sorter. The morphology of the sorted Gr-1^{high} cells, after staining with Wright-Giemsa stain, was observed with a Zeiss Axio Imager A1 microscope. Scale bar = 10 μm.

Figure 5 illustrates the extensive ingestion of PLGA NPs by the Gr-1^{high} cells and internalization into vesicles (Fig. 5b), in contrast to the untreated PBS control cells (Fig. 5a). These data demonstrate the highly phagocytic capabilities of Gr-1^{high} cells.

Proliferation of OT-I CD8^{+} T Cells and Upregulation of the SIINFEKL-MHC I-H2K[b] Complex After Co-Culture with PLGA/OVA NP-primed Gr-1^{high} Cells

Dye dilution assays have been widely used to analyze the proliferation of activated T cells (37). To examine the effect of PLGA/OVA NP-primed Gr-1^{high} cells on the activation of CD8^{+} T cells, negatively selected OT-I CD8^{+} T cells were labeled with 5 μM CFSE tracking dye and co-cultured for 72 h with Gr-1^{high} cells, pre-treated overnight with PBS, 10 μg/ml OVA, 100 μg/ml PLGA NPs, or 100 μg/ml PLGA/OVA NPs, and analyzed by flow cytometry. Figure 6 shows the proliferation of activated OT-I CD8^{+} T cells after co-culture with PLGA/OVA NP-primed Gr-1^{high} cells (Fig. 6a), and the activated T cells undergo proliferation and display enhanced light scattering parameters such as FSC-A, FSC-H, and FSC-W (Fig. 6a) compared to the PBS control (Fig. 6b), suggesting enlarged cell size and activation of
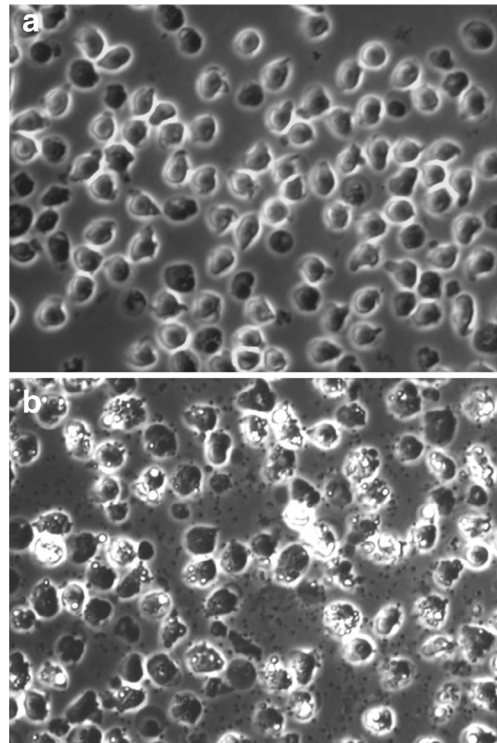
Fig. 5 Ingestion of PLGA/OVA NPs by Gr-1^{high} cells after 24 h of incubation, resulting in formation of invagination vesicles. Gr-1^{high} cells were sorted from bone marrow of femurs and tibiae of naive C57BL/6 J mice and treated with either (**a**) PBS or (**b**) PLGA/OVA NPs, incubated for 24 h at 37°C, and photographed using a Axiovert 200 M inverted microscope equipped with digital camera.

Fig. 6 Flow cytometric analysis of activated OT-I CD8$^+$ T cells. Two-parameter flow cytometric analysis was displayed, showing the proliferation and division of CFSE-labeled OT-I CD8$^+$ cells (**a**) co-cultured with PLGA/OVA-NP-primed Gr-1^{high} cells or (**b**) in PBS. (**c**) Upregulation of the expression of CD25 and CD69 in OT-I CD8$^+$ T cells after co-culture with Gr-1^{high} cells pretreated with PBS, OVA, PLGA NPs, or PLGA/OVA NPs. (**d**) Upregulation of expression of SIINFEKL-H-2K^b of MHC I complex on CD11b$^+$Gr-1^{high} cells, detected with 25-D1.16 mAb, after treatment with PLGA/OVA NPs for 48 h, compared to other control groups.
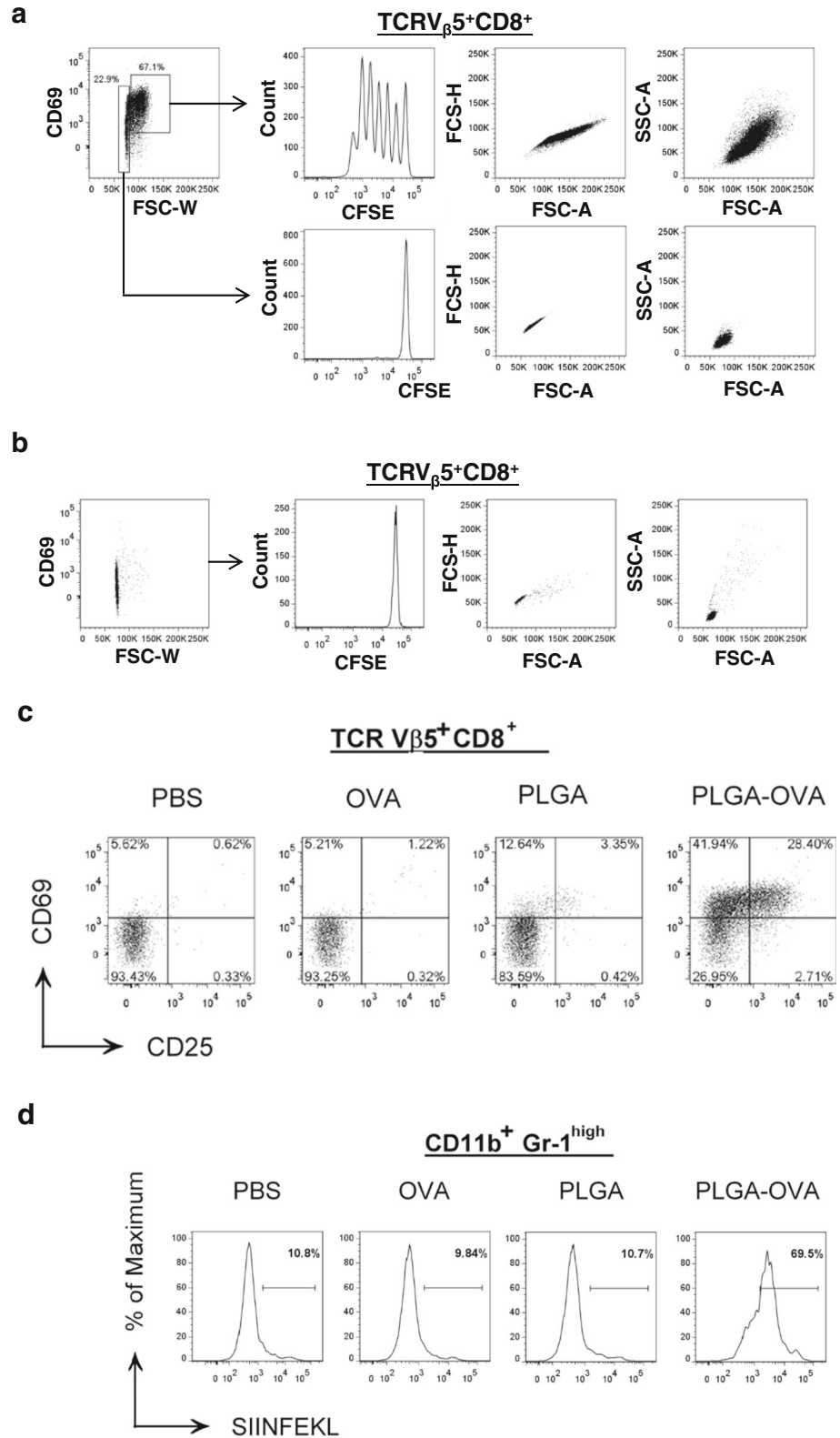
OT-I CD8$^+$ T cells after co-culture with PLGA/OVA NP-primed Gr-1^{high} cells. Almost all FSC-W$^+$ cells exhibit enhanced FSC-A/FSC-H light scattering signals and cell division. Co-culture with Gr-1^{high} cells also upregulated the expression of activation markers, such as CD25 and CD69, in OT-I CD8$^+$ T cells (Fig. 6c).

Treatment of Gr-1^{high} cells with PLGA/OVA NPs resulted in upregulation of the SIINFEKL-H2K[b] complex when detected with 25-D1.16, the monoclonal antibody reacting with the OVA-derived peptide (257–264; SIINFEKL) bound to H-2K[b] of MHC class I (Fig. 6d). These data showed that treatment of Gr-1^{high} cells with PLGA/OVA NPs induced cross-presentation of H-2K[b] binding OVA(257–264)-peptide (SIINFEKL) in contrast to other control groups (Fig. 6d).

Comparison of *In Vitro* Proliferation of OT-I CD8^{+} T Cells, After Co-Culture with Nanoparticles Treated BMDCs or Gr-1^{high} Subset

To compare T cell activation and proliferation induced by the PLGA/OVA NPs-treated antigen presenting cells (APCs), either day 6 BMDCs or Lin2⁻CD11b^{+}Gr-1^{high}-Ly-6C^{low} (Gr-1^{high}) cells were co-cultured with CFSE-labeled OT-I CD8^{+} T cells, followed by treatment with PBS, OVA, PLGA NPs, or PLGA/OVA NPs. Cells were harvested 72 h later and analyzed with a BD FACSVerse. Day 6 BMDCs appear to exhibit a higher antigen presentation capability than that of the Gr-1^{high} subset from bone marrow, leading to a higher T cell proliferation (59.9% vs. 40.6%) (Fig. 7).

Microscopic Examination of Activated OT-I CD8^{+} T Cells, After Co-Culture with the PLGA/OVA NP-primed Gr-1^{high} Cells

Gr-1^{high} cells were sorted by FACS, pre-treated with or without PLGA/OVA NPs, and incubated at 37°C for 16 h, followed by co-culture for 24 h with CD8^{+}TCRV$_\alpha$2^{+} T cells. Cells were sorted again by FACS, cytospun with a Cytospin4 slide centrifuge onto the glass slides, and stained

with Wright-Giemsa stain (Sigma-Aldrich), followed by observation with a Zeiss Axio Imager A1 microscope. Figure 8 shows the gating scheme and morphology of OT-I CD8^{+} T cells after co-culture with Gr-1^{high} cells treated with either PBS (Fig. 8a) or 100 µg/ml PLGA/OVA NPs (Fig. 8b). Activated OT-I CD8^{+} T cells, following activation by the PLGA/OVA NP-primed Gr-1^{high} cells, exhibit a larger size with larger nuclei and thicker enclosure of cytoplasm compared to the PBS control cells.

Analysis of Cell Cycles by BrdU Labeling

The thymidine analog 5-bromo-2′-deoxyuridine (BrdU) has been used to determine the turnover rate of T cells and B cells, where cells containing BrdU can be detected *in vitro* using flow cytometry after staining with fluorochrome-labeled anti-BrdU antibody (38). The sorted Gr-1^{high} cells were treated with PBS, 10 µg/ml OVA, 100 µg/ml PLGA NPs, or 100 µg/ml PLGA/OVA NPs and co-cultured for 48 h with the negatively selected OT-I CD8^{+} T cells, followed by treatment with 10 µM BrdU for another 24 h. Cells were then stained with 7-AAD and anti-BrdU-APC antibody, followed by flow cytometric analysis. Figure 9 showed that the percentages of CD3^{+}CD8^{+} T cells in the S and G2/M phases of the cell cycle in the PLGA/OVA NP-treated group are 40.1 and 7.378%, respectively, which are considerably higher than those of the control groups treated with PBS, OVA, or PLGA NPs (Fig. 9). These data illustrate immunomodulation of PLGA/OVA NPs on cell division of CD3^{+}CD8^{+} T cells via the Gr-1^{high} subset.

Induction of Gr-1^{high} Cell Apoptosis and Necrosis by PLGA/OVA NPs

To determine if PLGA/OVA NP treatment induces cell death of antigen presenting cells (APCs) and effector T cells, sorted Gr-1^{high} cells were pre-treated with PLGA/OVA NPs for 16 h and co-cultured with negatively selected OT-I CD8^{+} cells for 24, 36, 48, 60, and 72 h, followed by staining with CD8-APC-Cy7, Gr-1-APC, Annexin V-PE, and 7-AAD and analysis with a BD FACSVerse cytometer (BD Bioscience). Figure 10a shows the gating scheme for Gr-1^{high} and OT-I CD8^{+} T cells in the co-culture. The percentages of apoptotic/necrotic cells in the OT-I CD8^{+} T population were relatively reduced due to the proliferation of CD8^{+} T cells, activated by the Gr-1^{high} subset (Fig. 10b). The percentages of necrotic/late apoptotic cell death in OT-I CD8^{+}TCRVα2^{+} T cells were 31.3, 22.6, 26.8, and 31.7% at 36, 48, 60, and 72 h after co-culture, respectively, in the PLGA/OVA NP-treated group, which are significantly less than those values for the PBS control
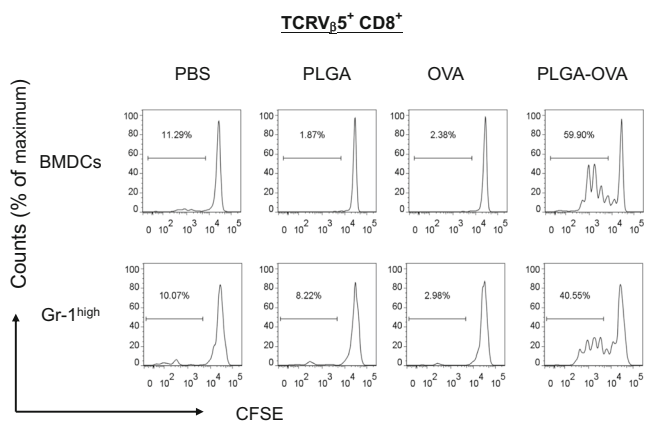
Fig. 7 *In vitro* OT-I CD8^{+} T cell proliferation. Day 6 bone marrow-derived dendritic cells (BMDCs) or freshly sorted Gr-1^{high} subset were co-cultured at 1:1 in the 96-well plates with CFSE-labeled OT-I CD8^{+} T cells, followed by treatment with PBS, OVA, PLGA NPs, or PLGA/OVA NPs. Cells were harvested 72 h later and analyzed by flow cytometry.
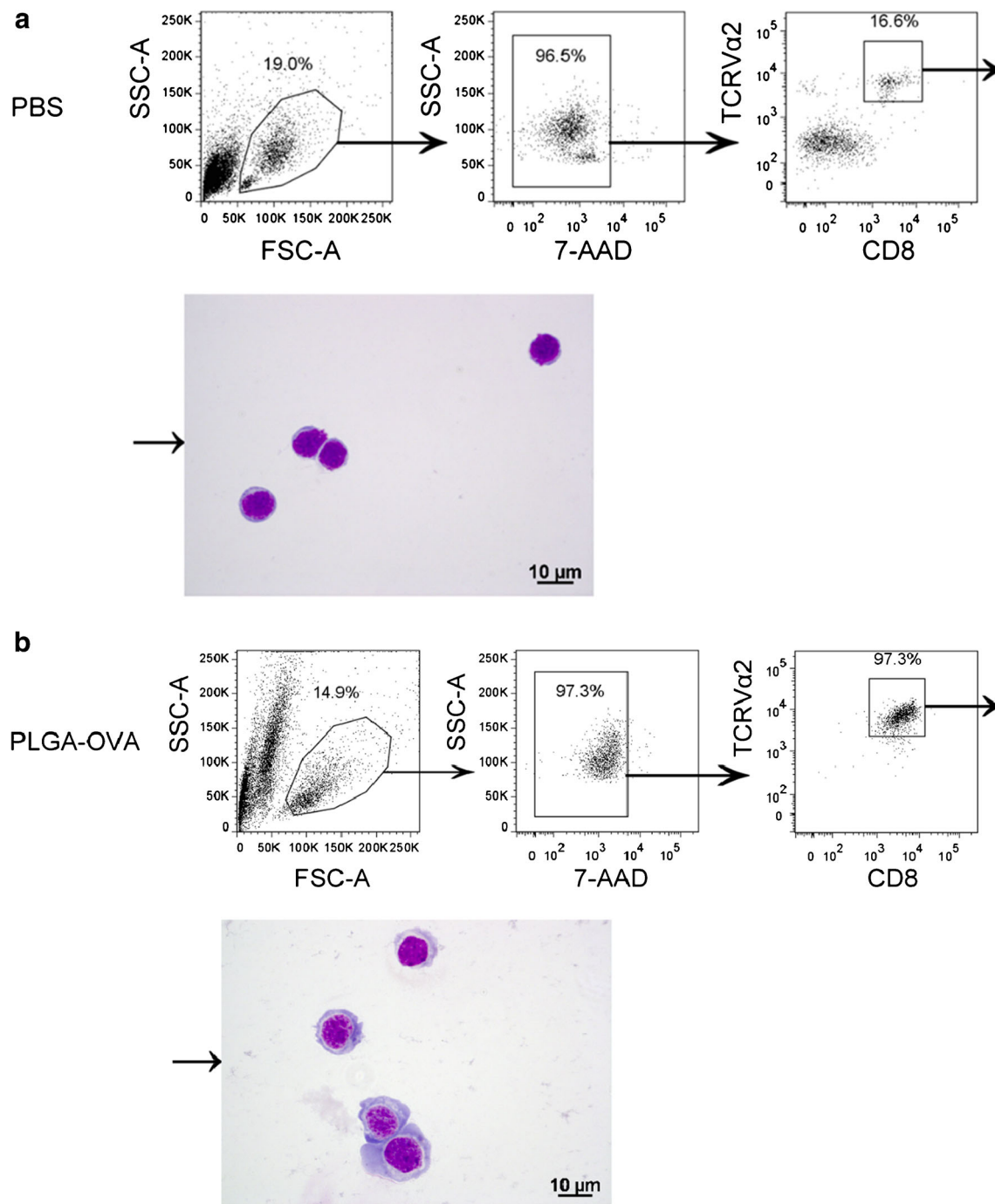
Fig. 8 Morphology of OT-I CD8^{+} Tcells activated by PLGA/OVA NP-primed Gr-1^{high} cells *in vitro*. The sorted Gr-1^{high} cells were treated with (**a**) PBS or (**b**) PLGA/OVA NPs for 16 h and co-cultured with OT-I CD8^{+} Tcells for 72 h. The OT-I CD8^{+} TCRVα2^{+} Tcells were then sorted by FACS, cytospun, and stained with Wright-Giemsa stain, followed by examination with a Zeiss Axio Imager A1 fluorescence microscope.

cells, showing 60.9, 61.6, 76.6, and 63.4%, respectively (Fig. 10b).

On the other hand, Gr-1^{high} cells undergo significant programmed cell death, including early apoptosis and necrosis, upon treatment with PLGA/OVA NPs. Figure 10c illustrates a significantly higher frequency of time-dependent apoptotic and necrotic cell death in the Gr-1^{high} population in the

PLGA/OVA NPs-treated group compared to the PBS control group (Fig. 10c). The degree of apoptosis and necrosis was shown to depend on the time of exposure to the NPs. Microscopic examination after staining Gr-1^{high} cells with Wright-Giemsa stain illustrated the apoptotic/necrotic cell morphology upon ingestion of the PLGA/OVA NPs (Fig. 10d). These data demonstrate that ingestion of PLGA/OVA NPs induced
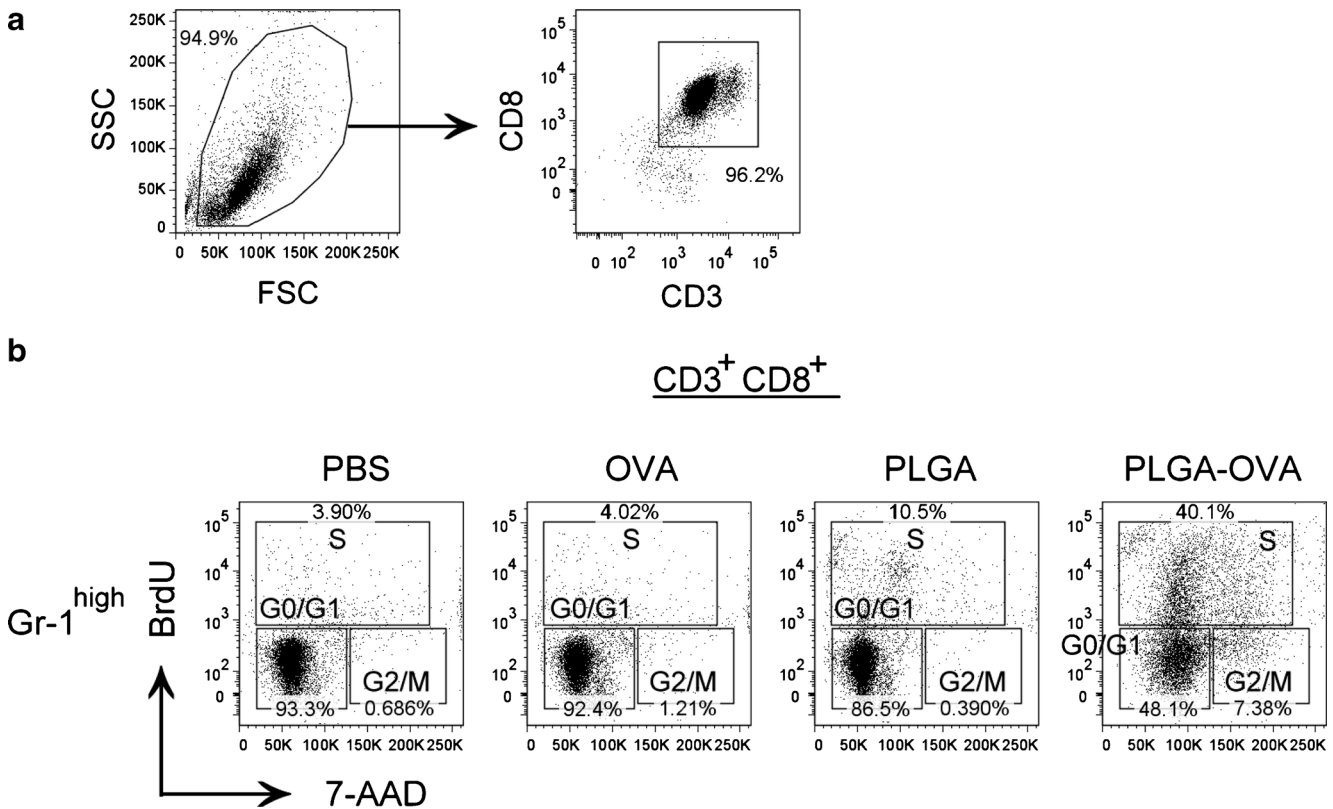
Fig. 9 Cell cycle analysis by staining OT-I CD8^{+} cells with 7-AAD and anti-BrdU antibody, followed by flow cytometric analysis. The sorted Gr-1^{high} cells were treated with PBS, 10 μg/ml OVA, 100 μg/ml PLGA NPs, or 100 μg/ml PLGA/OVA NPs for 16 h, and co-cultured for 48 h with negatively selected OT-I CD8^{+} T cells. Cells were then treated with 10 μM BrdU and incubated for another 24 h, stained with 7-AAD and anti-BrdU-APC antibody, and analyzed by flow cytometry, as described in Materials and Methods.

time-dependent programmed cell death in the Gr-1^{high} subset and promoted proliferation of antigen-specific OT-I CD8^{+} cells.

DISCUSSION

Activation of antigen-specific CD8^{+} T cell response plays important roles in the development of cancer immunotherapy and cancer-based vaccination. During the past few years of studies on nanoparticle-based antigen delivery, dendritic cells (DCs) received the most attention and have been considered the most potent antigen presenting cells for the induction of adaptive immunity; these cells therefore have become the major targets in most studies on anti-tumor immunotherapy and in the development of cancer vaccines to control immunity (39–42). The roles of polymorphonuclear neutrophils (PMN), the first line of defense against infective agents, in antigen delivery have unfortunately been largely ignored. The CD11b^{+}Gr-1^{high} subset of cells from mouse bone marrow were employed in this study to examine the capability of antigen presentation in nanoparticle-based vaccination to activate CD8^{+} T cells in OT-I mice that exhibit a higher sensitivity to antigen stimulation due to the involvement of selective

expansion of clones with higher affinity T cell receptors (TCRs). PLGA-NPs, which have been extensively investigated in recent years for delivery of soluble antigens for stimulation of antigen-specific cellular response against cancer, were employed in this study as a carrier to target the CD11b^{+}Gr-1^{high} subset from mouse bone marrow for the induction of MHC class I-mediated T cell activation.

The forward light scattering signal width (FSC-W), a parameter previously used to discriminate cell doublets, has been shown to be associated with proliferation of activated human T cells (43). Activation of T cells can be characterized by an increase in the forward light scattering signal width (FSC-W), a cytometric parameter used to discriminate cell doublets. Figure 6 shows that co-culture with PLGA/OVA NP-primed Gr-1^{high} cells induced the activation and *in vitro* proliferation of OT-I CD8^{+} T cells (Fig. 6a), in contrast to the PBS control group (Fig. 6b), resulting in an increase of the scattering signals of FSC-A, FSC-H, and FSC-W (Fig. 6a) and upregulation of the activation markers and expression of the SIINFEKL-MHC I-H2K[b] complex (Figs. 6c–d). Consequently, all proliferating cells are FSC-W^{+}. These results were further confirmed by microscopic examination of the morphological changes of OT-I CD8^{+} T cells, whereas the OT-I CD8^{+} T cells activated by PLGA/OVA NP-primed Gr-1^{high} cells
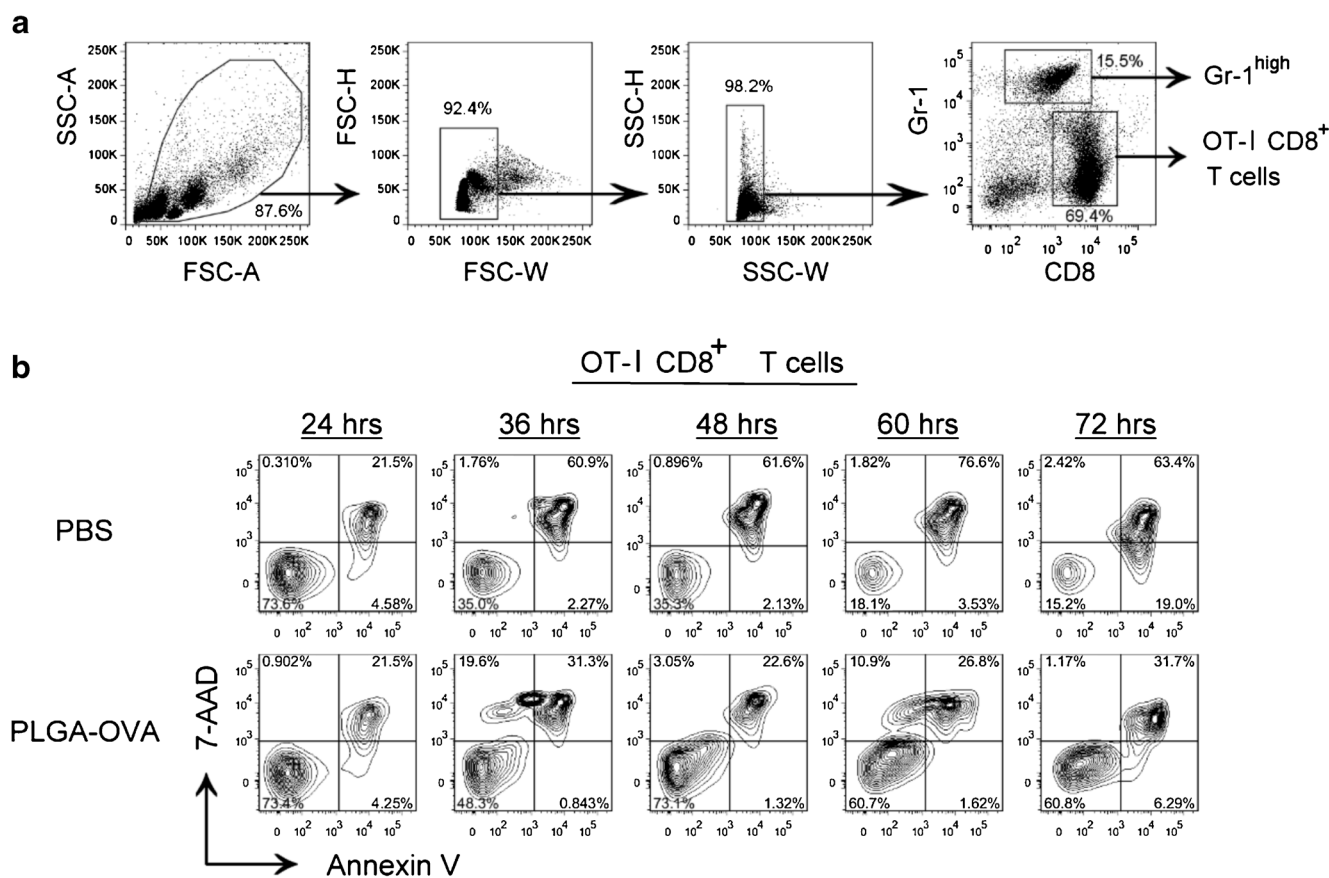
Fig. 10 Induction of apoptosis and necrosis in the co-culture of PLGA/OVA NP-primed Gr-1^{high} cells and OT-I CD8$^+$ T cells after incubation for 24, 36, 48, 60, and 72 h. Cells were stained with CD8-APC-Cy7, Gr-1-APC, Annexin V-PE, and 7-AAD, and analyzed by flow cytometry. (**a**), The gating scheme of CD11b$^+$Gr-1^{high} cells and OT-I CD8$^+$ T cells in the co-culture. (**b–c**), Flow cytometric analysis of apoptosis and necrosis of OT-I CD8$^+$ T cells (**b**) and Gr-1^{high} cells (**c**) in the co-culture. (**d**), Photomicrographs showing the morphology of CD11b$^+$Gr-1^{high} cells at 24, 48, and 72 h after treatment with PLGA/OVA NPs.

exhibited relatively abundant cytoplasm and enlarged large nuclei (Fig. 8b), compared to cells in the resting stage, which show the nucleus surrounded by a thin enclosure of cytoplasm in the PBS control (Fig. 8a). In parallel, the activation of OT-I CD8$^+$ T cells also induces cells to synthesize DNA and promotes entrance into the S and G2/M phases (Fig. 9).

Temporal analysis of treatment with PLGA/OVA NPs showed the induction of programmed cell death, such as apoptosis and necrosis, in Gr-1^{high} cells after ingestion of polymeric NPs (Fig. 10c), whereas CD8$^+$ T cells undergo extensive proliferation after co-culture with the Gr-1^{high} subset (Fig. 10b). As a result, the degree of cell death was relatively reduced in the T cell population in the PLGA NPs/OVA-treated group, compared to the untreated PBS control. These data not only illustrate that PLGA/OVA NPs are able to activate antigen-specific CD8$^+$ T cells mediated by the bone marrow Gr-1^{high} subset but also showed exposure time-dependent cell apoptosis and necrosis in PLGA/OVA NP-treated Gr-1^{high} cells.

Data presented in this study demonstrate that PLGA/OVA NP-primed Gr-1^{high} cells are able to activate

OT-I CD8$^+$ T cells, suggesting that the Gr-1^{high} polymorphonuclear subset may serve as antigen presenting cells (APCs) in nanoparticle-based vaccination. The results obtained in this study raise the potential of employing PLGA/OVA NPs as the vaccine adjuvant, targeting the bone marrow Gr-1^{high} subset and possibly also including the blood polymorphonuclear cells, the most abundant leukocytes in the peripheral circulation, to induce a cellular immune response.

CONCLUSIONS

The development of effective vaccine delivery is crucially important in vaccine-based cancer therapy, and biodegradable nanoparticles have emerged as a promising approach to enhance cellular immunity in immunization strategies. We have demonstrated in this study the feasibility of employing PLGA/OVA NPs-treated CD11b$^+$Gr-1^{high} subset in the murine bone marrow for cross-presentation of exogenous antigens and

c

d
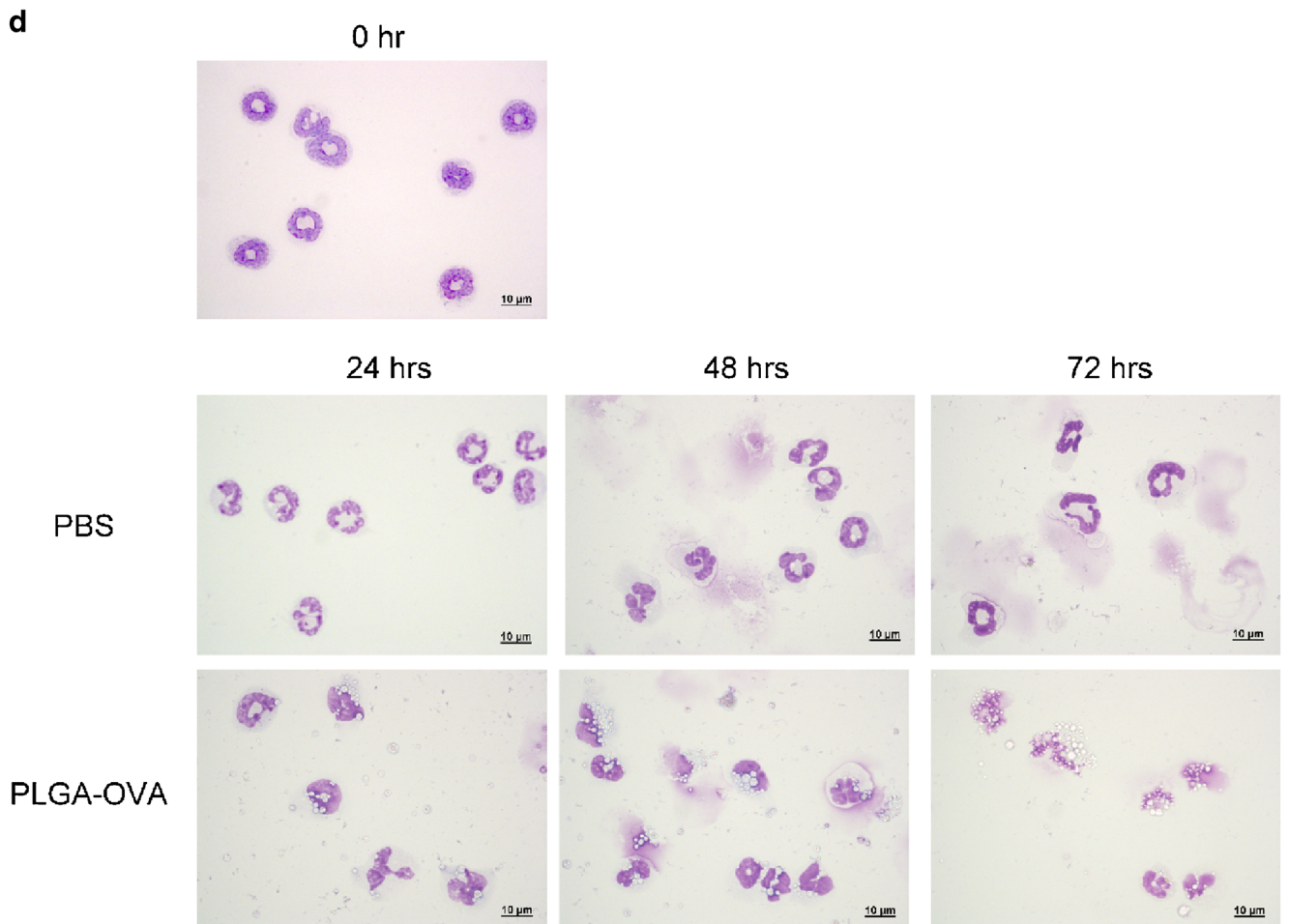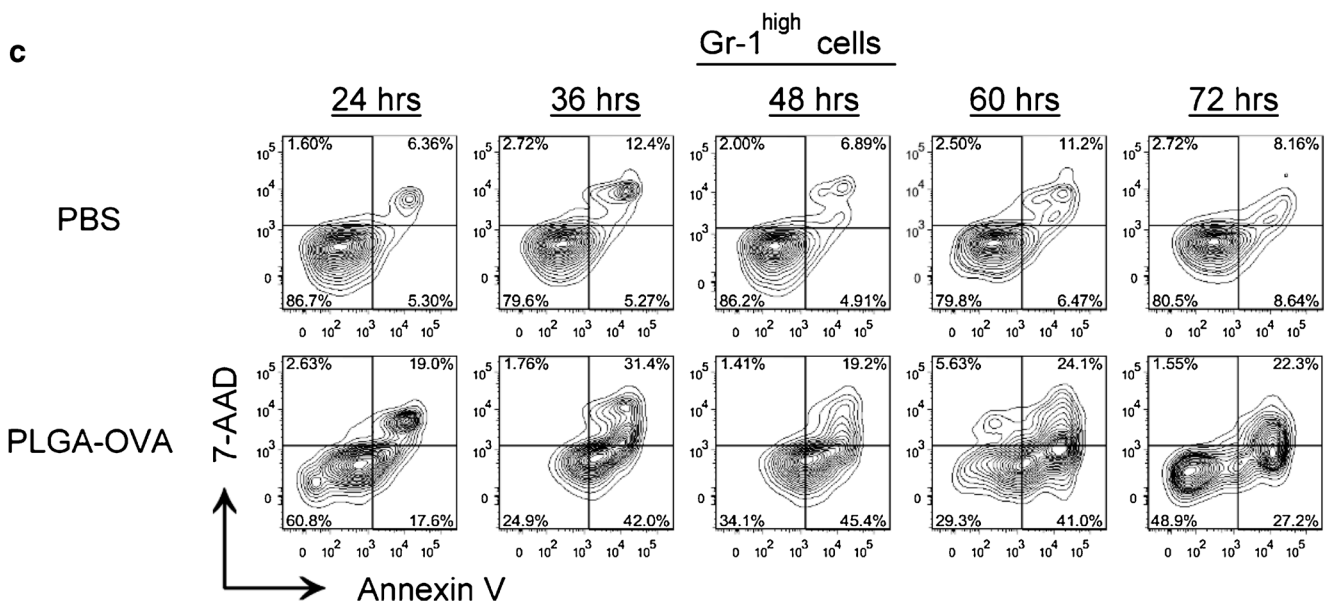
Fig. 10 (continued)

activation of antigen-specific CD8^{+} T cell activation *in vitro*, promoting the ensuing proliferation and cell cycle modulation, and induction of programmed cell death of the APCs.

ACKNOWLEDGMENTS AND DISCLOSURE

REFERENCES

1. Gonzalez PA, Carreno LJ, Coombs D, Mora JE, Palmieri E, Goldstein B, et al. T cell receptor binding kinetics required for T cell activation depend on the density of cognate ligand on the antigen-presenting cell. Proc Natl Acad Sci U S A. 2005;102: 4824–9.

2. Li H, Li Y, Jiao J, Hu HM. Alpha-alumina nanoparticles induce efficient autophagy-dependent cross-presentation and potent antitumour response. Nat Nanotechnol. 2011;6:645–50.

3. Lebel ME, Daudelin JF, Chartrand K, Tarrab E, Kalinke U, Savard P, et al. Nanoparticle adjuvant sensing by TLR7 enhances CD8+ T cell-mediated protection from Listeria monocytogenes infection. J Immunol. 2014;192:1071–8.

4. Cruz LJ, Rosalia RA, Kleinovink JW, Rueda F, Lowik CW, Ossendorp F. Targeting nanoparticles to CD40, DEC-205 or CD11c molecules on dendritic cells for efficient CD8 T cell response: a comparative study. J Control Release. 2014;192C:209–18.

5. Silva AL, Rosalia RA, Varypataki E, Sibuea S, Ossendorp F, Jiskoot W. Poly-(lactic-co-glycolic-acid)-based particulate vaccines: particle uptake by dendritic cells is a key parameter for immune activation. Vaccine. 2015;33:847–54.

6. Hubbell JA, Thomas SN, Swartz MA. Materials engineering for immunomodulation. Nature. 2009;462:449–60.

7. Steenblock ER, Fahmy TM. A comprehensive platform for ex vivo T-cell expansion based on biodegradable polymeric artificial antigen-presenting cells. Mol Ther. 2008;16:765–72.

8. Raghuwanshi D, Mishra V, Suresh MR, Kaur K. A simple approach for enhanced immune response using engineered dendritic cell targeted nanoparticles. Vaccine. 2012;30:7292–9.

9. Hirosue S, Kourtis IC, van der Vlies AJ, Hubbell JA, Swartz MA. Antigen delivery to dendritic cells by poly(propylene sulfide) nanoparticles with disulfide conjugated peptides: cross-presentation and T cell activation. Vaccine. 2010;28:7897–906.

10. Hamdy S, Elamanchili P, Alshamsan A, Molavi O, Satou T, Samuel J. Enhanced antigen-specific primary CD4+ and CD8+ responses by codelivery of ovalbumin and toll-like receptor ligand monophosphoryl lipid A in poly(D, L-lactic-co-glycolic acid) nanoparticles. J Biomed Mater Res A. 2007;81:652–62.

11. Amoozgar Z, Goldberg MS. Targeting myeloid cells using nanoparticles to improve cancer immunotherapy. Advanced drug delivery reviews. 2015;91:38–51.

12. Trombetta ES, Mellman I. Cell biology of antigen processing in vitro and in vivo. Annu Rev Immunol. 2005;23:975–1028.

13. Reddy ST, Swartz MA, Hubbell JA. Targeting dendritic cells with biomaterials: developing the next generation of vaccines. Trends in immunology. 2006;27:573–9.

14. Palucka K, Banchereau J. Dendritic-cell-based therapeutic cancer vaccines. Immunity. 2013;39:38–48.

15. Biermann H, Pietz B, Dreier R, Schmid KW, Sorg C, Sunderkotter C. Murine leukocytes with ring-shaped nuclei include granulocytes, monocytes, and their precursors. Journal of leukocyte biology. 1999;65:217–31.

16. Mellman I, Turley SJ, Steinman RM. Antigen processing for amateurs and professionals. Trends Cell Biol. 1998;8:231–7.

17. Steinman RM, Inaba K, Turley S, Pierre P, Mellman I. Antigen capture, processing, and presentation by dendritic cells: recent cell biological studies. Hum Immunol. 1999;60:562–7.

18. den Haan JM, Bevan MJ. Antigen presentation to CD8+ T cells: cross-priming in infectious diseases. Current opinion in immunology. 2001;13:437–41.

19. Beauvillain C, Delneste Y, Scotet M, Peres A, Gascan H, Guermonprez P, et al. Neutrophils efficiently cross-prime naive T cells in vivo. Blood. 2007;110:2965–73.

20. Shen SS, Yang YW. Antigen delivery for cross priming via the emulsion vaccine adjuvants. Vaccine. 2012;30:1560–71.

21. Lyons AB. Analysing cell division in vivo and in vitro using flow cytometric measurement of CFSE dye dilution. J Immunol Methods. 2000;243:147–54.

22. Lyons AB, Hasbold J, Hodgkin PD. Flow cytometric analysis of cell division history using dilution of carboxyfluorescein diacetate succinimidyl ester, a stably integrated fluorescent probe. Methods Cell Biol. 2001;63:375–98.

23. Soares A, Govender L, Hughes J, Mavakla W, de Kock M, Barnard C, et al. Novel application of Ki67 to quantify antigen-specific in vitro lymphoproliferation. J Immunol Methods. 2010;362:43–50.

24. Sun Y, Sun Y, Lin G, Zhang R, Zhang K, Xie J, et al. Multicolor flow cytometry analysis of the proliferations of T-lymphocyte subsets in vitro by EdU incorporation. Cytometry Part A. 2012;81: 901–9.

25. Holm M, Thomsen M, Hoyer M, Hokland P. Optimization of a flow cytometric method for the simultaneous measurement of cell surface antigen, DNA content, and in vitro BrdUrd incorporation into normal and malignant hematopoietic cells. Cytometry Part A. 1998;32:28–36.

26. Yang YW, Hsu PY. The effect of poly(D, L-lactide-co-glycolide) microparticles with polyelectrolyte self-assembled multilayer surfaces on the cross-presentation of exogenous antigens. Biomaterials. 2008;29:2516–26.

27. Coombes AG, Yeh MK, Lavelle EC, Davis SS. The control of protein release from poly(DL-lactide co-glycolide) microparticles by variation of the external aqueous phase surfactant in the water-in oil-in water method. J Control Release. 1998;52:311–20.

28. Fu K, Harrell R, Zinski K, Um C, Jaklenec A, Frazier J, et al. A potential approach for decreasing the burst effect of protein from PLGA microspheres. J Pharm Sci. 2003;92:1582–91.

29. Saadati R, Dadashzadeh S, Abbasian Z, Soleimanjahi H. Accelerated blood clearance of PEGylated PLGA nanoparticles following repeated injections: effects of polymer dose, PEG coating, and encapsulated anticancer drug. Pharm Res. 2013;30:985–95.

30. Wu CA, Yang YW. Induction of cell death by saponin and antigen delivery. Pharm Res. 2004;21:271–7.

31. Mosmann T. Rapid colorimetric assay for cellular growth and survival: application to proliferation and cytotoxicity assays. J Immunol Methods. 1983;65:55–63.

32. Kruisbeek AM. Isolation of mouse mononuclear cells. Current protocols in immunology / edited by John E Coligan [et al.]. Chapter 3:Unit 3 1 (2001).

33. Liu K, Victora GD, Schwickert TA, Guermonprez P, Meredith MM, Yao K, et al. In vivo analysis of dendritic cell development and homeostasis. Science. 2009;324:392–7.

34. Inaba K, Inaba M, Romani N, Aya H, Deguchi M, Ikehara S, et al. Generation of large numbers of dendritic cells from mouse bone marrow cultures supplemented with granulocyte/macrophage colony-stimulating factor. J Exp Med. 1992;176:1693–702.

35. Shen SS, Yang YW. Dynamics of antigen delivery and the functional roles of L121-adjuvant. Vaccine. 2015:4341–4348.

36. Bossuyt X, Marti GE, Fleisher TA. Comparative analysis of whole blood lysis methods for flow cytometry. Cytometry. 1997;30:124–33.

37. Muul LM, Silvin C, James SP, Candotti F. Measurement of proliferative responses of cultured lymphocytes. Current protocols in immunology / edited by John E Coligan [et al.]. Chapter 7:Unit 7 10 11–17 10 24 (2008).

38. Tough DF, Sprent J, Stephens GL. Measurement of T and B cell turnover with bromodeoxyuridine. Current protocols in immunology / edited by John E Coligan [et al.]. Chapter 4:Unit 4 7 (2007).

39. Haddadi A, Hamdy S, Ghotbi Z, Samuel J, Lavasanifar A. Immunoadjuvant activity of the nanoparticles' surface modified with mannan. Nanotechnology. 2014;25:355101.

40. Jimenez-Perianez A, Abos Gracia B, Lopez Relano J, Diez-Rivero CM, Reche PA, Martinez-Naves E, et al. Mesoporous silicon microparticles enhance MHC class I cross-antigen presentation by human dendritic cells. Clin Dev Immunol. 2013;2013:362163.

41. Palucka K, Banchereau J. SnapShot: cancer vaccines. Cell. 2014;157:516–516 e511.

42. Steinman RM. Dendritic cells in vivo: a key target for a new vaccine science. Immunity. 2008;29:319–24.

43. Bohmer RM, Bandala-Sanchez E, Harrison LC. Forward light scatter is a simple measure of T-cell activation and proliferation but is not universally suited for doublet discrimination. Cytometry Part A. 2011;79:646–52.